Understanding Solid-State Reactions of Organic Crystals with Density Functional Theory-Based Concepts

Shaoxin Feng and Tonglei Li*

514 College of Pharmacy, Pharmaceutical Sciences, University of Kentucky, 725 Rose Street, Lexington, Kentucky 40536

Received: April 15, 2005; In Final Form: June 16, 2005

Solid-state reactions are commonly observed in organic crystals, including pharmaceutical and agricultural materials, fine chemicals, dyes, explosives, optics, and many other substances. The fact that these reactions are in general highly anisotropic with regard to the initiation and propagation in a crystal has led to this study for investigating the effect of crystal packing on the reaction mechanism and kinetics of organic crystals. We have used electron density-based concepts, including nuclear Fukui function, developed from density functional theory, for elucidating the effect of electronic structures of different polymorphs on the difference in their chemical reactivity. Two polymorphs of flufenamic acid were studied. The calculation results on major reacting faces of the two forms support their reactivity difference with ammonia gas. In addition, we calculated surface energies of reacting faces to discuss how the mechanical difference may affect the propagation of solid-state reaction.

Introduction

Organic crystalline materials play a central role in pharmaceuticals, agrochemicals and fine chemicals. Most of pharmaceutical materials are molecular crystals. Organic crystals are also heavily involved in explosives, high-energy materials, dyes, and organic electronic and optic materials. Their physicochemical properties affect formulation and production, and have a huge impact on the performance and stability of products.[1,2]

Just like every compound in any other phase, organic crystals are susceptible to chemical degradation and reactions with other materials (gases, liquids, and solids). Because of their important pharmaceutical roles, such reactions may lead to severe consequences. A therapeutic substance or an excipient must be chemically stable during the manufacturing, storage, and administration stages. Any degradation or chemical incompatibility of drugs and excipients can cause serious side effects. Solid-state reactions of fine chemicals play an important role in other industries as well. Clearly, understanding, and subsequently predicting solid-state reactions will make a significant impact on materials science.

Typical solid-state reactions include oxidation, photochemical and thermal reactions. Gas−solid reactions are common. A solid-state reaction is generally regarded as a reaction where the crystalline phase is involved as a reagent. Five criteria have been suggested for determining whether a reaction is a true solid-state reaction.[1,3] In a broader sense, phase transformation and re/desolvation may be considered to be solid-state reactions as well. The electronic structures can be significantly changed when one polymorph transforms into another. The chemical compositions are also affected when solvent molecules move in or out of the host crystal. Therefore, the study of solid-state reactions is one of the essential tasks in solid-state chemistry and materials science.

* Corresponding author. Telephone: (859) 257-1472. Fax: (859) 257-7585. E-mail: tonglei@uky.edu.

In contrast to liquid/gas reactions, the chemical reactivity or stability of organic crystals is further complicated by polymorphism, i.e., the difference in the internal packing of the same molecules. Many examples have been reported where polymorphs of the same compound show variance in reactivity.[4−6] Moreover, of the same polymorph, the reactivity may be anisotropic with respect to crystal faces where chemical moieties are different. Reaction rates along particular crystallographic directions can be significantly varied.

Many types of solid-state reactions have been reported. Among them, gas−solid reactions have long been studied, initially focusing on metal and inorganic compounds when the stability of metals and alloys was not well understood. Reactions between crystals and oxygen,[7] ozone,[8] water vapor,[9] anhydrous chlorine gas,[10] and acetonitrile vapor [11] are some examples of gas−solid reactions that have been investigated. Pioneering studies of the solid-state reaction were conducted by Paul and Curtin on the acid−base type of solid−gas reaction, such as with ammonia gas by *p*-chlorobenzoic anhydride crystals.[3,12] It was often observed that certain crystal faces were attacked preferentially by gases and reactions propagated along specific directions. Two polymorphs (form I and form III) of flufenamic acid showed different reaction rates with ammonia gas,[6] and the reaction started on the (100) face of both polymorphs. Most interestingly, although the thermodynamic stability order switches at 42 °C between the two forms, the (100) face of form I always showed larger reaction rates than that of form III regardless of reaction temperature.

Current knowledge about solid-state reaction mechanisms is largely based on studies by the Curtin and Paul group three decades ago.[3,12−17] A four-step process was suggested for a solid-state reaction: (1) loosening of molecules on crystal surfaces, (2) chemical reaction, (3) formation of solid solution, and (4) phase separation of product. Molecular mobility was thought to be the deciding factor in loosening of molecules, and was focused on by many studies.[4,18−20] Nevertheless, the

10.1021/jp0519666 CCC: $30.25
Published on Web 07/21/2005

role of crystal packing has been mainly discussed from the geometric point of view including the topochemical postulate and reaction cavity.[21,22] Few studies of solid-state reactivity of organic crystals have been reported from the electronic level.

Clearly, solid-state reactions are much more complex than liquid reactions. The reaction is highly anisotropic and heterogeneous as the reaction always starts on the surface. Because of relatively weak intermolecular interactions, organic crystals are susceptive to polymorph formation.[23] In addition, crystal growth morphology is greatly varied under different growth conditions, such as solvents, additives, impurities, temperature, concentrations, etc.[24] Often observed, the kinetics of solid-state reactions can be considerably affected by polymorphism and growth morphology. Thus, our aim is to study the impact of molecular packing of different polymorphs on the chemical reactivity with electronic calculations.

Quantum mechanics (QM) and density functional theory (DFT) have tremendously advanced the molecular sciences, highlighted by the 1998 Nobel Prize to Kohn and Pople.[25,26] A huge interest in conceptual DFT has surged in the past decade, producing enlightening concepts and results.[27,28] A recent study by Luty et al. used DFT-based concepts to investigate the explosive mechanism of RDX (hexahydro-1,3,5-trinitro-1,3,5-triazine).[29] The molecule has three symmetrically equivalent N−N bonds, but only one bond breaks initially in the explosion. In the study, nuclear Fukui functions of the RDX molecule were calculated. These calculations indicated that the nuclear Fukui functions of one N−N bond were significantly larger than those of another two bonds, causing the C_3 symmetry of the three N−N bonds to break. Because a nuclear Fukui function represents the force applied on an atom due to electron transfer or perturbation, this study was able to provide significant insights into the explosive mechanisms of highly symmetric molecules, such as RDX. Nevertheless, the research was focused on the single molecule of RDX, not the crystalline state of the explosive.

In this report, we illustrate that the nuclear Fukui function may be used to characterize the difference in chemical reactivity of two polymorphs of flufenamic acid. In addition, we discuss the role of mechanical strength in the propagation of chemical reaction.

Methodology

DFT claims that energy is a functional of charge density.[25,30,31] As a molecular system changes from a ground state to another because of perturbations in electron population or the number of electrons, dN, as well as the external potential that is defined by atomic positions and nuclear charges, $\delta v(\mathbf{r})$, the expansion of the system energy change to second order may be expressed as[32,33]

$$dE = \underbrace{\left(\frac{\partial E}{\partial N}\right)_v}_{\mu} dN + \underbrace{\int \left[\frac{\delta E}{\delta v(\mathbf{r})}\right]_N}_{\rho(\mathbf{r})} dv(\mathbf{r})d\mathbf{r} + \underbrace{\frac{1}{2}\left(\frac{\partial^2 E}{\partial N^2}\right)_v}_{\eta} (dN)^2 + \underbrace{\int \left[\frac{\delta^2 E}{\delta v(\mathbf{r})\partial N}\right]}_{f(\mathbf{r})} dv(\mathbf{r})d\mathbf{r}\,dN + \frac{1}{2}\underbrace{\int \left[\frac{\delta^2 E}{\delta v(\mathbf{r})\delta v(\mathbf{r}')}\right]_N}_{\beta(\mathbf{r},\mathbf{r}')} dv(\mathbf{r})d\mathbf{r}\,dv(\mathbf{r}')d\mathbf{r}' \quad (1)$$

where $\mathbf{r}$ is the position vector, μ the electronic chemical potential (the opposite of the electronegativity[34]), characterizing electron's escape tendency from the equilibrium, $\rho(\mathbf{r})$ the charge density, η the hardness, $f(\mathbf{r})$ the Fukui function, and $\beta(\mathbf{r}, \mathbf{r}')$ the linear response function. The local Fukui function can be calculated from the change of the charge density as a response to the change of the number of electrons in a molecular system by[35]

$$f(\mathbf{r}) = \left[\frac{\delta^2 E}{\delta v(\mathbf{r})\partial N}\right] = \left[\frac{\delta \mu}{\delta v(\mathbf{r})}\right]_N = \left[\frac{\partial \rho(\mathbf{r})}{\partial N}\right]_v \quad (2)$$

Thus, Fukui function is capable of describing the sensitivity of a molecular system to electronic and nuclear perturbations.[36,37] The hardness has been proved to be related to Klopman's frontier molecular orbital theory,[38] calculated by the energy gap between ionization potential, I, and electron affinity, A,[39]

$$\eta = \frac{1}{2}\left(\frac{\partial^2 E}{\partial N^2}\right)_v = \frac{1}{2}\left(\frac{\partial \mu}{\partial N}\right)_v \cong \frac{I - A}{2} \quad (3)$$

The inverse of hardness is softness, S.[40] It is clear that μ, η, and S are global properties of a whole molecular system, while $\rho(\mathbf{r})$ and $f(\mathbf{r})$ are local ones. It is widely regarded that hardness indicates a resistance to charge transfer, while softness measures ease of transfer and is associated with polarizability.[25] DFT-based concepts and their combinations have been discussed in many applications including molecular properties (electrophilicity, aromaticity, conformation, etc.), reactivity and catalysis,[28] illustrating the theory that the electron density is the fundamental quantity for describing atomic and molecular ground states.[30]

Because hardness (η in eq 3) indicates resistance to the electron transfer, its dependence on molecular deformation, named as the nuclear stiffness, may be relevant in characterizing the chemical reactivity:[29,41]

$$\mathbf{G}_i = \left(\frac{\partial \eta}{\partial \mathbf{Q}_i}\right)_N \quad (4)$$

where $\mathbf{Q}_i = \mathbf{R}_i - \mathbf{R}_{i,0}$ is the displacement vector of atom i from its equilibrium position, $\mathbf{R}_{i,0}$. It can be calculated by the electronic force (i.e., Hellmann−Feynman force) acting on the atom:

$$\mathbf{G}_i = -\frac{1}{2}(\mathbf{F}_i^+ + \mathbf{F}_i^-) \quad (5)$$

Here $\mathbf{F}_i^+$ and $\mathbf{F}_i^-$ are forces on the same atom i when the number of its electrons has increased (+) or decreased (−) with its position fixed, respectively. Similarly, the nuclear reactivity index is defined as[42]

$$\Phi_i = -\left(\frac{\partial \mu}{\partial \mathbf{Q}_i}\right)_N = \left(\frac{\partial \mathbf{F}_i}{\partial N}\right)_{v(\mathbf{r})} = \frac{1}{2}(\mathbf{F}_i^+ - \mathbf{F}_i^-) \quad (6)$$

Like $\mathbf{F}_i^+$ and $\mathbf{F}_i^-$, $\mathbf{G}_i$ and Φ_i and are vectors, characteristic of each atom. Their contributions to the global hardness and chemical potential can be expressed as

$$\eta = \eta_0 + \sum_i \left(\frac{\partial \eta}{\partial \mathbf{Q}_i}\right)_N \cdot \mathbf{Q}_i = \eta_0 + \sum_i \mathbf{G}_i \cdot \mathbf{Q}_i$$

$$\mu = \mu_0 + \sum_i \left(\frac{\partial \mu}{\partial \mathbf{Q}_i}\right)_N \cdot \mathbf{Q}_i = \mu_0 - \sum_i \Phi_i \cdot \mathbf{Q}_i \quad (7)$$

where η_0 and μ_0 are the hardness and chemical potential of

undeformed molecules at equilibrium. Thus, contributions of $\mathbf{G}_i$ and Φ_i to the decrease of hardness and chemical potential as a reaction occurs can be revealed from their scalar products with atomic displacements (i.e., $\mathbf{G}_i \cdot \mathbf{Q}_i$ and $\Phi_i \cdot \mathbf{Q}_i$). It is possible to predict which atoms are involved in the reaction, whether the molecule accepts or donates electron(s), and whether the reacting bond is shortened or stretched.[41] It has been demonstrated that large absolute values of $\mathbf{G}_i$ and Φ_i can be used to identify those atoms and bonds that are involved in a chemical reaction.[29] Furthermore, from their relations with electronic forces of ionized species, they can reveal how much an atom participates in a reaction. A large force on an atom indicates a large displacement, resulting in a bond breaking, shortening or conformational change. In fact, the concept of nuclear reactivity index has been extended into so-called nuclear Fukui function:[42]

$$\Phi_i^+ = \left(\frac{\partial \mathbf{F}_i}{\partial N}\right)_{v(\mathbf{r})}^+ = \mathbf{F}_i^+ - \mathbf{F}_i^0$$
$$\Phi_i^- = \left(\frac{\partial \mathbf{F}_i}{\partial N}\right)_{v(\mathbf{r})}^- = \mathbf{F}_i^0 - \mathbf{F}_i^- \qquad (8)$$

to characterize a nucleophilic or electrophilic attack, respectively. For a molecule in equilibrium, $\mathbf{F}_i^0$ is close to zero. Thus, $\mathbf{F}_i^+$ or $\mathbf{F}_i^-$ alone may be able to study the reactivity of respective atoms in a nucleophilic or electrophilic reaction.[35]

Since a chemical reaction is driven by the change in system energy, and is accompanied by the electron transfer and atomic displacement, the nuclear Fukui function, a local function to describe system sensitivity to a simultaneous perturbation in electron number, N, and nuclear position, $\mathbf{R}$, may be useful for characterizing the reactivity of crystals with respect to crystal packing.

In addition, mechanical strength determines the propagation and reaction kinetics of solid-state reactions. As it is often observed that a solid-state reaction may proceed in a specific crystallographic direction, study of the mechanical properties on different faces may help understand the solid-state reaction. Thus, evaluation of surface energies of crystal faces may be helpful for comparing how the mechanical strength of different polymorphs affects the reaction kinetics. Surface energy of a face can be calculated by

$$E_{\text{surf}} = \frac{1}{2}\frac{(E_{\text{slab}} - nE_{\text{bulk}})}{S} \qquad (9)$$

where E_{slab} and E_{bulk} are total energies of the slab and bulk crystal, n is the thickness (or layers of unit cells) of the slab, and S the surface area. A slab is a 2D periodic structure representing a modeled crystal face.

In this study, electronic structures, nuclear Fukui functions and surface energies of two polymorphs of flufenamic acid, form I and form III, were calculated with a periodic ab initio program, Crystal 03.[43] Both Hartree−Fock (HF) and DFT with B3LYP exchange-correlation functional[44,45] were used. Pople's 6-21G and 6-31G basis sets were used for each calculation method. The (100) face of the two polymorphs were modeled, and their nuclear Fukui functions were analyzed for unraveling the difference in their chemical reactivities with ammonia gas.

Flufenamic acid, 2-[[3-(trifluoromethyl)phenyl]amino]benzoic acid, is an analgesic and antiinflammatory drug. Although six polymorphs have been determined, only form I (white, mp 134 °C) and form III (yellow, mp 128 °C) can be easily crystallized. Shown in Figure 1, both forms are monoclinic, and their

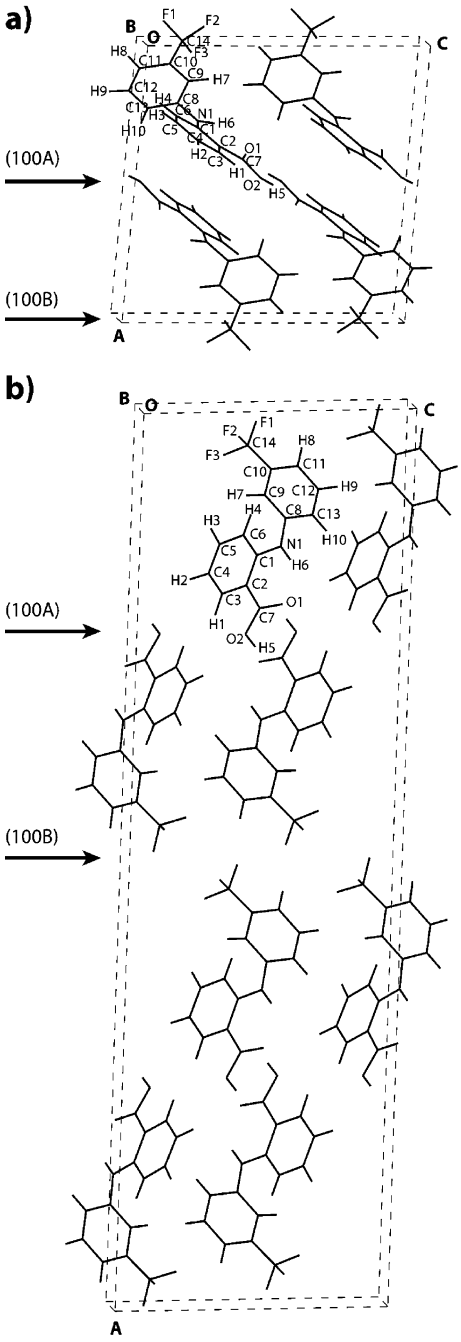

Figure 1. Crystal structures of form I (a) and form III (b) of flufenamic acid. Molecules of two forms are denoted with the same labels. The two different cuts, (100A) and (100B), are marked.

structures have been measured with single X-ray diffraction. Lattice parameters of form I ($P2_1/c$) are $a = 12.5$, $b = 7.9$, $c = 12.9$ Å, and $\beta = 95.2°$;[46] lattice parameters of form III ($C2/c$) are $a = 39.8$, $b = 5.1$, $c = 12.2$ Å, and $\beta = 92.5°$.[47] The bulk crystal structures were optimized with the same methods that were used to calculate nuclear Fukui functions. Lattice parameters were fixed during the optimization. Accordingly, slab models of (100) faces of both forms were built. For each form, there are two different crystallographic cuts of the (100) face. As shown in Figure 1, one slices through hydrogen bonds (denoted as (100A)), and another does not (denoted as (100B)). Carboxylic acid groups that react to ammonia are exposed on the (100A) cut. For building the (100) slabs of form III, a half of the unit cell along the a axis was considered as one layer due to the fact that the top four molecules in the unit cell (Figure

1) are only translationally related to the bottom four molecules by a vector (1/2*a*, 1/2*b*, *0*). Slab models of two cuts of each polymorph were subjected to quantum mechanical calculations. Since flufenamic acid deprotonates during the reaction with ammonia, Φ_i^+ was calculated (eq 8) for the analysis. $\mathbf{F}_i^0$ and $\mathbf{F}_i^+$ of each atom were obtained from calculations of the neutral and anionic forms, respectively, of a bulk or a slab model; the molecular structure of the anionic form was kept the same as its neutral counterpart.

Results and Discussion

Two polymorphs of flufenamic acid showed different reaction rates with ammonia gas.[6] It was observed that the reaction started on the (100) face of both polymorphs. After 24 h, both forms were totally reacted to form product salt crystals. However, form I showed much faster reacting rates than form III. In addition, the reaction order was not affected by the enantiotropic order of the two forms. At 60 °C, form I still reacted faster than form III, despite the stability transition temperature being at 42 °C.

Illustrated in Figure 2 are nuclear Fukui functions calculated on (100A) faces of two polymorphs of flufenamic acid. Because they are vectors, nuclear Fukui functions are drawn as arrows. The longer the arrows, the larger the functions are. Arrows are also color-coded from red to green to blue indicating their magnitudes from large to small. It can be seen that carboxylic group has the largest nuclear Fukui functions while other atoms have relatively small values. The quantitative results of nuclear Fukui functions of (100) faces are listed in Table 1. For the nucleophilic attack of crystal faces, such as by NH_3, calculations of anionic and neutral slabs were carried out. Because the program could not handle a partial extra charge, the anionic calculations of (100) slabs of form I and form III were conducted with one extra electron that was introduced to the unit cells of slab models. Figure 3 shows the face-integrated Fukui functions of slabs. A face-integrated Fukui function represents an average value of Fukui functions on a crystallographic plane that is parallel to the surface of a slab.[48] Since the Fukui function characterizes the increase in electron density for an anionic species (eq 2), Figure 3 indicates that the extra electron in the anionic slab models prefers to redistribute around the surface of the slabs. For the (100A) of both forms, there is almost no increase in electron density in the middle of slabs. There is some increase for the (100B) due to the −COOH in the middle. As a result, the nuclear Fukui functions were further normalized by the surface area of unit cells of the slab models (1.01 of form I, and 0.65 nm^2 of form III) to have the same surface charge transfer at 0.5 e/nm^2, and listed in Table 1. The normalization was based on the argument that the larger the electronic perturbation, the larger the Hellmann−Feynman force becomes. Because the electron redistribution occurs mainly on the surface, to maintain the same increase in the surface electron density for both form I and form III for meaningful comparisons, nuclear Fukui functions were normalized by considering the unit surface areas of the two forms. The normalization implies that both forms react with the same number of ammonia molecules per surface area so that the numbers of electrons transferred during the reactions are equivalent.

It is clearly illustrated from Figure 1 and Table 1 that nuclear Fukui functions of the carboxylic group of the (100A) of both forms are much larger than those of other atoms. In addition, the nuclear Fukui functions of the −COOH of the (100A) slab where the functional group is exposed are greater than those of the (100B) slabs where the −COOH is positioned in the middle.

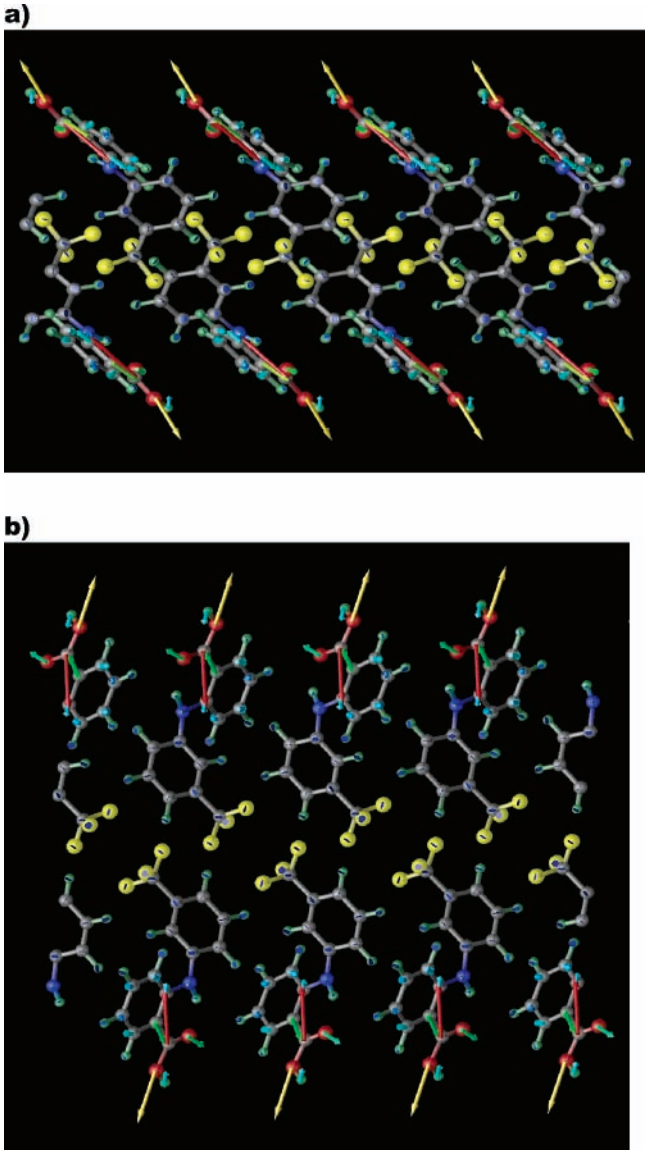

Figure 2. The (100A) face of form I (a) and form III (b) of flufenamic acid. Nuclear Fukui functions are color-coded and shown as arrows whose lengths and directions denote magnitudes and directions of the vectors. Two movies of both rotatable models are available as Supporting Information.

Although the $-CF_3$ of the (100B) also show significantly large values of nuclear Fukui functions, it is unlikely for the $-CF_3$ to participate in the chemical reaction with NH_3. The calculation results of the single molecule (Table 1) clearly show that the −COOH has relatively large values of nuclear Fukui function while the $-CF_3$ has very small ones, indicating that the reaction should involve the −COOH, not the $-CF_3$. The large values of the $-CF_3$ of the (100B) slabs are caused by the large electronic perturbations on the surface (Figure 3). Furthermore, normalized nuclear Fukui functions of the −COOH of form I are significantly larger than those of form III. Table 2 also lists the normalized nuclear Fukui functions that were calculated by different computational methods, indicating the consistency of relative scales of nuclear Fukui functions. Effects of the layer thickness of slab models on the nuclear Fukui functions were tested as well. Little changes (less than 2%) of their values (not shown) were observed when four layers were used for building the slabs and calculations of the nuclear Fukui functions.

Nuclear Fukui function characterizes how much physical stress may be applied to a nucleus because of the change in

TABLE 1: Calculated Nuclear Fukui Functions of the (100A) and (100B) Slab Models of Form I and Form III of Flufenamic Acid with the B3LYP/6-31G[a]

		form I				form III			
		(100A)		(100B)		(100A)		(100B)	
	single molecule	original	normalized	original	normalized	original	normalized	original	normalized
C1	2.384	0.584	0.592	0.858	0.869	0.540	0.337	0.705	0.441
C2	4.043	1.216	1.231	0.448	0.454	1.478	0.924	0.299	0.187
C3	1.728	0.476	0.482	0.158	0.161	0.638	0.399	0.091	0.057
C4	0.941	0.182	0.185	0.189	0.192	0.321	0.201	0.077	0.048
C5	1.446	0.463	0.469	0.532	0.539	0.335	0.210	0.286	0.179
C6	1.529	0.443	0.449	0.620	0.628	0.328	0.205	0.414	0.259
C7	5.436	2.062	2.089	0.627	0.635	2.995	1.872	0.378	0.236
C8	2.304	0.045	0.046	0.585	0.593	0.024	0.015	0.951	0.595
C9	0.631	0.016	0.016	0.275	0.279	0.021	0.013	0.247	0.155
C10	0.941	0.020	0.020	0.734	0.743	0.037	0.023	0.945	0.591
C11	0.917	0.029	0.030	0.184	0.186	0.031	0.020	0.537	0.336
C12	0.531	0.033	0.034	0.238	0.241	0.011	0.007	0.304	0.190
C13	1.343	0.042	0.042	0.203	0.205	0.041	0.026	0.446	0.279
C14	1.725	0.019	0.019	2.426	2.458	0.007	0.004	3.118	1.949
F1	0.443	0.009	0.009	1.061	1.074	0.005	0.003	1.430	0.894
F2	0.539	0.007	0.007	0.676	0.685	0.003	0.002	0.912	0.570
F3	0.651	0.004	0.004	0.606	0.614	0.002	0.001	0.715	0.447
H1	0.062	0.093	0.095	0.009	0.009	0.075	0.047	0.015	0.009
H2	0.206	0.113	0.114	0.025	0.026	0.066	0.041	0.014	0.009
H3	0.145	0.015	0.015	0.051	0.052	0.023	0.014	0.038	0.024
H4	0.146	0.009	0.009	0.068	0.069	0.011	0.007	0.045	0.028
H5	0.527	0.423	0.428	0.058	0.059	0.648	0.405	0.025	0.016
H6	0.460	0.072	0.073	0.190	0.193	0.079	0.050	0.191	0.119
H7	0.067	0.004	0.004	0.107	0.109	0.006	0.004	0.081	0.051
H8	0.069	0.003	0.003	0.120	0.122	0.004	0.003	0.094	0.059
H9	0.109	0.012	0.012	0.084	0.085	0.002	0.001	0.092	0.058
H10	0.130	0.047	0.047	0.021	0.021	0.014	0.009	0.037	0.023
N1	2.070	0.153	0.155	0.841	0.852	0.084	0.052	0.995	0.622
O1	3.936	1.154	1.168	0.719	0.728	1.196	0.748	0.489	0.306
O2	2.964	1.649	1.670	0.368	0.373	2.532	1.583	0.199	0.124

[a] Bulk crystal structures that were used to build slab models were optimized with the B3LYP/6-21G. The normalization was based on the unit surface areas of two forms. Results of single molecule by B3LYP/6-31G//B3LYP/6-21G are also listed. C7, O1, O2, and H5 belong to −COOH. Unit: nN.

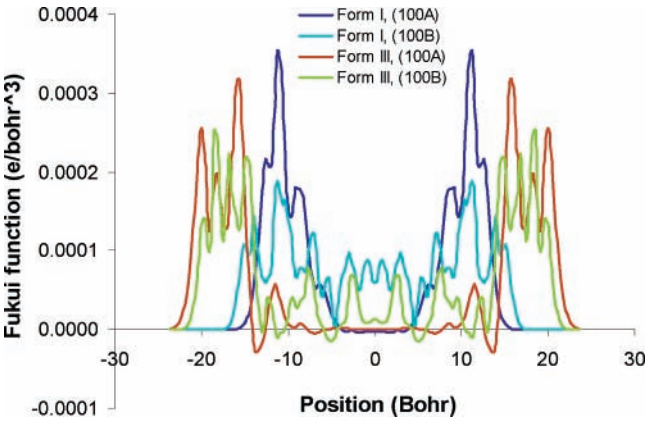

Figure 3. Face-integrated Fukui functions of the (100A) and (100B) slab models of form I and form III of flufenamic acid. Slabs of form I were of one unit-cell thickness. Slabs of form III were of half-unit-cell thickness.

electronic structures (eq 8). It is expected that large physical stresses on nuclei lead to breaking of chemical bonds. The calculations of the (100) slabs of form I and form III of flufenamic acid obviously show that, during a nucleophilic attack such as by ammonia gas, the −COOH functional groups are most affected. The large forces on −COOH may initiate changes of chemical bonds. The difference of calculation results between the (100A) and (100B) indicates that the (100A) cut is most likely the reactive surface. The difference of nuclear Fukui functions between the (100A) and (100B) of each form is reminiscent of how much electronic perturbation can affect the nuclear Fukui function. The little change in electron density of the middle region in the (100B) cuts (Figure 3) shows a minimal impact on nuclear Fukui function of the −COOH. More importantly, the results suggest that form I is more reactive than form III. The larger nuclear Fukui functions of the −COOH of the (100A) of form I reveal that the −COOH is under significantly greater stresses than the −COOH of form III, and should be more reactive. Considering the fact that form I reacted much faster than form III, the normalized nuclear Fukui functions may be capable of describing the reactivity of a crystal face.

To elucidate the influence of mechanical strength on chemical reactivity, surface energies of the slab models were calculated. Calculated by the DFT/6-31G with the B3LYP functional, surface energy values are 0.242 of the (100A), 0.171 of the (100B) of form I, 0.454 of the (100A), and 0.137 J/m^2 of the (100B) of form III, respectively. The surface energy of the (100A) of each form is larger than that of the (100B), very likely due to the hydrogen bonding between −COOH groups of the (100A) cuts. In addition, the (100A) of form III has a significantly larger surface energy than of form I, indicating a tighter binding of the (100A) face of form III. As the reaction starts on the (100) face of each polymorph, its propagation and penetration into the bulk are expected to be limited by the intermolecular binding strength. As it is the energy used to maintain a unit area of surface, surface energy characterizes the intermolecular interactions within a crystallographic plane, specifying the mechanical strength. Therefore, the larger surface energy of the (100A) of form III may contribute to its slower

TABLE 2: Calculated Nuclear Fukui Functions of the (100A) Slab Models of Form I and Form III of Flufenamic Acid with Different Methods[a]

	HF/6-21G		HF/6-31G		B3LYP/6-21G		B3LYP/6-31G	
	form I	form III	form I	form III	form I	form III	form I	form III
C1	0.799	0.553	0.803	0.542	0.633	0.364	0.592	0.337
C2	1.901	1.361	1.966	1.410	1.316	0.953	1.231	0.924
C3	0.920	0.714	0.896	0.701	0.567	0.443	0.482	0.399
C4	0.429	0.381	0.396	0.359	0.215	0.222	0.185	0.201
C5	0.958	0.406	0.978	0.395	0.506	0.230	0.469	0.210
C6	0.754	0.396	0.798	0.390	0.488	0.228	0.449	0.205
C7	2.657	2.373	2.757	2.423	2.052	1.809	2.089	1.872
C8	0.048	0.029	0.053	0.027	0.044	0.015	0.046	0.015
C9	0.026	0.009	0.018	0.005	0.017	0.013	0.016	0.013
C10	0.038	0.027	0.015	0.021	0.018	0.024	0.020	0.023
C11	0.044	0.030	0.028	0.020	0.030	0.020	0.030	0.020
C12	0.045	0.022	0.038	0.014	0.037	0.007	0.034	0.007
C13	0.052	0.025	0.055	0.019	0.045	0.025	0.042	0.026
C14	0.025	0.008	0.028	0.009	0.022	0.005	0.019	0.004
F1	0.012	0.004	0.014	0.004	0.010	0.003	0.009	0.003
F2	0.015	0.003	0.015	0.003	0.010	0.002	0.007	0.002
F3	0.004	0.001	0.004	0.003	0.003	0.001	0.004	0.001
H1	0.122	0.061	0.098	0.065	0.090	0.049	0.095	0.047
H2	0.132	0.054	0.121	0.050	0.118	0.042	0.114	0.041
H3	0.023	0.017	0.015	0.019	0.015	0.015	0.015	0.014
H4	0.016	0.010	0.014	0.009	0.012	0.008	0.009	0.007
H5	0.505	0.486	0.456	0.450	0.393	0.398	0.428	0.405
H6	0.116	0.062	0.101	0.051	0.075	0.067	0.073	0.050
H7	0.008	0.005	0.005	0.006	0.004	0.004	0.004	0.004
H8	0.002	0.002	0.002	0.003	0.003	0.003	0.003	0.003
H9	0.021	0.003	0.015	0.002	0.015	0.001	0.012	0.001
H10	0.067	0.013	0.055	0.011	0.051	0.011	0.047	0.009
N1	0.246	0.126	0.227	0.120	0.163	0.063	0.155	0.052
O1	1.379	0.905	1.445	0.944	1.080	0.683	1.168	0.748
O2	1.756	1.712	1.734	1.674	1.598	1.488	1.670	1.583

[a] Bulk crystal structures that were used to build slab models were optimized with the HF/6-21G and B3LYP/6-21G when slabs were calculated with the HF and DFT methods, respectively. The results were normalized with regard to the unit surface areas. C7, O1, O2, and H5 belong to −COOH. Unit: nN.

reaction rate than that of form I. The surface energy results also suggest that the reaction of both forms may undergo a layer-by-layer process because the nonreacting (100B) cuts have much smaller surface energy values than the (100A). The reaction propagating through the (100A) should be much faster than the reaction penetrating the (100) face. For single crystals of flufenamic acid, the (100B) cut of each form is expected dominant on the (100) face because of smaller surface energies. The reactive (100A) may exist as imperfection or defect sites on the (100) face, initiating and spreading the chemical reaction. If a crystal has more surface defects, the vertical penetration toward the bulk may contribute more to the overall reaction kinetics.

Conclusions

The difference in the solid-state reaction of two polymorphs of flufenamic acid, form I and form III, was elucidated by studying their electronic structures, particularly the nuclear Fukui functions, and their mechanical properties. Results suggest that nuclear Fukui functions are capable of describing the influence of crystal packing on the solid-state reactivity. Moreover, because of the highly heterogeneous nature of a solid-state reaction, mechanical properties need to be considered in understanding solid-state reactions. Considering that the −COOH of form I is more reactive as well as that form III is mechanically stronger, our calculations support experimental observations of the reaction kinetics of flufenamic acid with ammonia gas.

Acknowledgment. We thank Dr. Shubin Liu (UNC-Chapel Hill) for constructive discussions of density functional theory. This work was supported by NSF (CTS-0303945 and DMR-0449633).

Supporting Information Available: Movies (.avi) of nuclear Fukui functions of flufenamic acid. This material is available free of charge via the Internet at http://pubs.acs.org.

References and Notes

(1) Morawetz, H. *Science* **1966**, *152*, 705.
(2) Byrn, S. R.; Pfeiffer, R. R.; Stowell., J. G. *Solid-State Chemistry of Drugs*, 2nd ed.; SSCI, Inc.: West Lafayette, IN, 1999.
(3) Paul, I. C.; Curtin, D. Y. *Acc. Chem. Res.* **1973**, *6*, 217.
(4) Byrn, S. R.; Sutton, P. A.; Tobias, B.; Frye, J.; Main, P. *J. Am. Chem. Soc.* **1988**, *110*, 1609.
(5) Chen, X. M.; Morris, K. R.; Griesser, U. J.; Byrn, S. R.; Stowell, J. G. *J. Am. Chem. Soc.* **2002**, *124*, 15012.
(6) Chen, X. M.; Li, T. L.; Morris, K. R.; Byrn, S. R. *Mol. Cryst. Liq. Cryst.* **2002**, *381*, 121.
(7) Scheffer, J. R.; Ouchi, M. D. *Tetrahedron Lett.* **1970**, 223.
(8) Desvergne, J. P.; Thomas, J. M. *J. Chem. Soc., Perkin Trans. 2* **1975**, 584.
(9) Ahlneck, C.; Zografi, G. *Int. J. Pharm.* **1990**, *62*, 87.
(10) Lamartin, R.; Perrin, R. *J. Org. Chem.* **1974**, *39*, 1744.
(11) Scott, J. L. *J. Chem. Soc., Perkin Trans. 2* **1995**, 495.
(12) Paul, I. C.; Curtin, D. Y. *Science* **1975**, *187*, 19.
(13) Lin, C. T.; Paul, I. C.; Curtin, D. Y. *J. Am. Chem. Soc.* **1974**, *96*, 3699.
(14) Lin, C. T.; Curtin, D. Y.; Paul, I. C. *J. Am. Chem. Soc.* **1974**, *96*, 6199.
(15) Miller, R. S.; Curtin, D. Y.; Paul, I. C. *J. Am. Chem. Soc.* **1974**, *96*, 6329.
(16) Miller, R. S.; Paul, I. C.; Curtin, D. Y. *J. Am. Chem. Soc.* **1974**, *96*, 6334.
(17) Miller, R. S.; Curtin, D. Y.; Paul, I. C. *J. Am. Chem. Soc.* **1974**, *96*, 6340.
(18) Byrn, S. R.; Kessler, D. W. *Tetrahedron* **1987**, *43*, 1335.
(19) Byrn, S. R.; Lin, C. T. *J. Am. Chem. Soc.* **1976**, *98*, 4004.
(20) Byrn, S. R. *J. Pharm. Sci.* **1976**, *65*, 1.
(21) Schmidt, G. M. J. *J. Chem. Soc.* **1964**, 2014.
(22) Cohen, M. D. *Angew. Chem., Int. Ed. Engl.* **1975**, *14*, 386.
(23) Hollingsworth, M. D. *Science* **2002**, *295*, 2410.
(24) Bennema, P. *J. Cryst. Growth* **1996**, *166*, 17.
(25) Kohn, W.; Becke, A. D.; Parr, R. G. *J. Phys. Chem.* **1996**, *100*, 12974.
(26) Pople, J. A. *Angew. Chem., Int. Ed.* **1999**, *38*, 1894.
(27) Nalewajski, R. F. *Adv. Quantum Chem.* **2003,** *43*, 119.
(28) Geerlings, P.; De Proft, F.; Langenaeker, W. *Chem. Rev.* **2003**, *103*, 1793.
(29) Luty, T.; Ordon, P.; Eckhardt, C. J. *J. Chem. Phys.* **2002**, *117*, 1775.
(30) Hohenberg, P.; Kohn, W. *Phys. Rev. B* **1964**, *136*, B864.
(31) Parr, R. G.; Yang, W. T. *Annu. Rev. Phys. Chem.* **1995**, *46*, 701.
(32) Nalewajski, R. F. *Comput. Chem.* **2000**, *24*, 243.
(33) Parr, R. G.; Yang, W. *Density-Functional Theory of Atoms and Molecules*; Oxford University Press: New York, 1989.
(34) Parr, R. G.; Donnelly, R. A.; Levy, M.; Palke, W. E. *J. Chem. Phys.* **1978**, *68*, 3801.
(35) De Proft, F.; Liu, S. B.; Geerlings, P. *J. Chem. Phys.* **1998**, *108*, 7549.
(36) Ayers, P. W.; Parr, R. G. *J. Am. Chem. Soc.* **2001**, *123*, 2007.
(37) Ayers, P. W.; Parr, R. G. *J. Am. Chem. Soc.* **2000**, *122*, 2010.
(38) Klopman, G. *J. Am. Chem. Soc.* **1968**, *90*, 223.
(39) Parr, R. G.; Pearson, R. G. *J. Am. Chem. Soc.* **1983**, *105*, 7512.
(40) Yang, W. T.; Parr, R. G. *Proc. Natl. Acad. Sci. U.S.A.* **1985**, *82*, 6723.
(41) Ordon, P.; Komorowski, L. *Chem. Phys. Lett.* **1998**, *292*, 22.
(42) Cohen, M. H.; Gandugliapirovano, M. V.; Kudrnovsky, J. *J. Chem. Phys.* **1994**, *101*, 8988.
(43) Doll, K.; Saunders, V. R.; Harrison, N. M. *Int. J. Quantum Chem.* **2001**, *82*, 1.
(44) Becke, A. D. *Phys. Rev. A* **1988**, *38*, 3098.
(45) Lee, C. T.; Yang, W. T.; Parr, R. G. *Phys. Rev. B* **1988**, *37*, 785.
(46) Murthy, H. M. K.; Bhat, T. N.; Vijayan, M. *Acta Crystallogr. B* **1982**, *38*, 315.
(47) McConnell, J. F. *Cryst. Struct. Commun.* **1973**, *2*, 459.
(48) Li, T.; Liu, S.; Feng, S.; Aubrey, C. E. *J. Am. Chem. Soc.* **2005**, *127*, 1364.